

Electron impact ionization of 1-butanol: I. Mass spectra and partial ionization cross sections

Item Type	Journal article
Authors	Pires, W.A.D.;Nixon, K.L.;Ghosh, S.;Amorim, R.A.A.;Neves, R.F.C.;Duque, H.V.;da Silva, D.G.M.;Jones, D.B.;Brunger, M.J.;Lopes, M.C.A.
Citation	Pires, WAD., Nixon, KL., Ghosh, S., Amorim, RAA., Neves, RFC., Duque, HV., da Silva, DGM., Jones, DB., Brunger, MJ., Lopes, MCA. (2018) 'Electron impact ionization of 1-butanol: I. Mass spectra and partial ionization cross sections' International Journal of Mass Spectrometry, 430 pp. 158-167 doi: 10.1016/j.ijms.2018.03.011
DOI	10.1016/j.ijms.2018.03.011
Publisher	Elsevier
Journal	International Journal of Mass Spectrometry
Download date	2026-06-18 14:43:21
License	https://creativecommons.org/licenses/by-nc-nd/4.0/
Link to Item	http://hdl.handle.net/2436/621329

Electron Impact Ionization of 1-Butanol: I. Mass Spectra and Partial Ionization Cross Sections

W. A. D. Pires¹, K. L. Nixon^{1,2}, S. Ghosh¹, R. A. A. Amorim¹, R. F. C. Neves^{1,3}, H. V. Duque¹, D. G. M. da Silva¹, D. B. Jones⁴, M. J. Brunger⁴ and M. C. A. Lopes^{1*}

¹ Departamento de Física, Universidade Federal de Juiz de Fora, Juiz de Fora, MG, 36936-900, Brazil

² School of Sciences, University of Wolverhampton, Wolverhampton WV1 1LY, UK

³ Instituto Federal do Sul de Minas Gerais, Campus Poços de Caldas, Minas Gerais, Brazil

⁴ College of Science and Engineering, Flinders University, GPO Box 2100, Adelaide SA 5001, Australia

* corresponding author: cristina.lopes@ufjf.edu.br

Abstract

Experimental measurements of the cations created through electron impact ionization have been undertaken for the primary isomer of butanol, using a Hiden Quadrupole Mass Spectrometer (EPIC 300) with a mass resolution of 1 amu. The mass spectrum recorded at an incident electron energy of 70 eV, normalized and placed on an absolute scale, reveals the relative probability of forming 76 different cations of butanol by either direct ionization or dissociative ionization. Individual partial ionization cross sections (PICS) for the 38 main cationic fragments, measured at electron energies in the range 10-100 eV, are also reported for the first time in this work.

PACS numbers: 34.80.Ht, 34.80.Gs

Keywords: Mass spectra, direct ionization and dissociative ionization, partial ionization cross sections.

1. Introduction

Fossil fuels are an essential part of our lives, having significant applications in industries, power generation and transportation. Although the utilization of these energy sources has been very important for the development of humanity, our dependence on fossil fuels has been increasingly questioned over the last decade or so [1-2]. Among the issues raised about the intensive use of petroleum-based fuels, are the emission of greenhouse gasses and the environmental impact involved in their production and use. In this context, research into biofuels has been enhanced in order to allow for the efficient replacement of fossil fuels. One aspect of this research has involved investigating the plasma pre-treatment of renewable organic material, such as sugar cane, in order to enhance the production of useful chemicals, including alcohols, which are

widely used [3-4]. The advantage of using organic plants as feedstock for fuels over petrochemicals is that their use becomes a largely carbon neutral process [3]. One of the most promising alcohols that might be used as an alternative fuel is 1-butanol [5]. This is due to the fact that butanol has an energy density of 33.1 MJ/Kg, and is therefore more economical for vehicles than ethanol (~ 26.9 MJ/Kg) [6]. While the octane number of the isomers of butanol (87-104 AKI) [7-8] is lower than that of ethanol (99.5 AKI) and gasoline (85-96 AKI), it is of a sufficient value to be used in internal combustion engines, in order to produce spontaneous combustion. Consequently using 1-butanol, in principle, means there is no loss of mechanical efficiency [5,6,9]. Furthermore, 1-butanol can replace gasoline without the need for any material modifications to the engine components [6] which represents another advantage to its use. Finally, we note that as 1-butanol can be produced from genetically manipulated algae and fermentation of renewable biomass [5,6,9,10] it represents an environmentally friendly alternative to fossil fuels.

The potential of 1-butanol for application as an economic fuel has attracted the attention of the scientific community, as shown by both the theoretical [11-13] and experimental [9,11,14-16] works that have been published. An experimental and theoretical investigation reporting the absolute total ionization cross sections (TICS) for the butanol isomers was published by Hudson *et al.* [11] in the energy range of 16 - 207 eV. Independently, Zavilopulo *et al.* [15] reported on a study of dissociative ionization of some of the alcohols, including the determination of relative partial ionization cross sections (PICS) and mass spectra (MS) for 1-butanol. Other works observed in the literature pertain to both experimental [12,16] and theoretical [12-13] investigations into elastic differential, integral and momentum transfer cross sections for scattering from butanol isomers. In the studies published by Khakoo *et al.* [12] for 1-butanol and by Fedus *et al.* [16] for isobutanol, the elastic electron-scattering cross sections were obtained for the energy range of 1-100 eV and at scattering angles from 5° to 130°, from which the integral elastic and momentum transfer cross sections were derived. There has also been work undertaken on 1-butanol by the dissociative electron attachment (DEA) community [17]. While the work of Ibănescu and Allan [17] clearly shows resonance enhanced ion yields for the OH⁻ and (M-1)⁻ anions, those results are only relative, so that the importance of this scattering channel cannot yet be ascertained. Thus, there remains a lack of cross section data in relation to electron scattering from 1-butanol, which the present investigation seeks to address, at least in part. In attempting to model the plasma process connected with the fuel ignition system of an engine, in order to improve and optimize that system's performance, complete and accurate electron impact cross section data bases [18] are required (such as are available for some species in LXCaT [19]). Clearly much further work is needed for 1-butanol, regarding vibrational excitation, electronic-state excitation and total cross sections, as well as absolute DEA data, before such a data base might be assembled for simulation studies involving 1-butanol.

This study is an extension of our previous investigations [20,21] into electron scattering from primary alcohols. The structure of the remainder of this manuscript is as follows. The experimental details and analysis methods are described in section 2, while both the relative and absolute mass spectrum and our PICS for 38 fragments are presented in section 3. The present data are also compared, where possible, with those currently available in the literature and discussed in this section. Finally, some conclusions from this investigation are drawn in section 4. Total ionisation cross sections, also derived from our measurements and calculated using the Binary-encounter Bethe (BEB) and an independent atom model with screening corrected additivity rule (IAM -SCAR) methods, are presented in a companion paper [22]

2. Experimental Methods and Data Analysis

Our apparatus has previously been described [20,21], and so only a brief précis of its main features is given here. The present electron impact ionization experiments with 1-butanol were performed using a Hiden Analytical [23] quadrupole mass spectrometer (QMS), fitted with a RF head capable of measuring masses up to 300 amu (EPIC 300) with 1 amu resolution. This spectrometer has an ionization stage and so can be operated in a residual gas analysing (RGA) mode, which was utilised in this investigation. The internal ionization source, with an energy spread of ~ 660 meV [21], was used to create ions by electron impact direct ionization and dissociative ionization. The ions were created from the uniform background of 1-butanol molecules, which effused from a needle positioned perpendicular to the axis of the mass filter and below the entrance to the ionization stage. The present study was carried out in the single collision regime, as verified by the linearity of the detected cation signals as a function of both the incident electron current and the 1-butanol pressure. This is explicitly demonstrated in figure 1 for the electron current range 10-20 μA (see figure 1a) and the 1-butanol pressure range 6.1×10^{-7} - 1.9×10^{-6} Torr (see figure 1b). For the results presented in section 3, however, a stable electron current of 20 μA and an operating pressure of $\sim 1.5 \times 10^{-6}$ Torr were employed. No mass dependence of the QMS over the mass range studied here was found, as was investigated in some detail by Nixon *et al.* [20]. Our previous studies also demonstrated that the extraction optics were capable of capturing all of the cations, regardless of their kinetic energy. The behaviour of the apparatus was verified by measurement of the PICS for Ar^+ , over the energy range of 10–100 eV. That data was compared to the corresponding results from Rejoub *et al.* [24], with excellent agreement being found. This therefore demonstrated that appropriate calibration of the spectrometer had been achieved.

The sample of 1-butanol, acquired from Sigma Aldrich with a spectrometric grade (99.5%), was stored in a vacuum flask and degassed by several freeze-pump-thaw cycles before the vapour was admitted into the vacuum chamber using a needle valve (MLV-22 [25]). The gas handling

lines were heated to ~ 40 °C, in order to prevent condensation of the vapour along the lines, and so yield a stable operating pressure. Here we note that the vacuum chamber itself did not require baking and remained at the ambient temperature of the air-conditioned laboratory i.e. 22 °C. The vapour pressure of 1-butanol was calculated to be 5.32 Torr, using the Antoine equation [20], where the constants employed were $A=4.54607$, $B=1351.555$ and $C = -93.34$ [26]. That pressure was considered to be sufficient to undertake our measurements.

Mass spectra for 1-butanol were measured on various days. After subtracting a measured mass spectra for the residual background gases, the spectra were combined to generate a true mass spectrum of 1-butanol. This mass spectrum was subsequently renormalized by setting the abundance of the most intense fragment, mass 31 amu, to 100 percent. The results from this process are shown in table 1, where 76 cationic fragments were observed. The standard deviations on the relative cation abundances were determined after the normalisation process. The mass spectrum shown in figure. 2 were set on an absolute scale, using the sum of all fragment ions observed, normalised to the TICS absolute value of Hudson *et al.* [11]. Note that as Hudson *et al.* did not actually report a TICS at 70 eV, that value was determined by an interpolation of the data they reported at 69 eV and 73 eV. The results from that normalisation process are also summarised in table 2 and figures 3 and 4, where a comparison to our earlier methanol, ethanol and 1-propanol results [20,21], where possible, is provided. The energy dependence of the PICS, for each of the main 38 cationic fragments we detected, between 10–100 eV, was also measured in this investigation. Those data were placed on an absolute scale using one point normalisation at 70 eV to the correspondent PICS value obtained in our absolute mass spectrum. The error bars in the 70 eV PICS were obtained by the square root of the square of the statistical error on our mass spectrum measurement, added to the square of the total error of the 70 eV TICS of Hudson *et al.* [11]. The results from this process are summarised in table 3 and figure 5, and we reiterate our belief that they represent the first absolute PICS to be reported for 1-butanol in the literature.

The sum of all the PICS in table 3 or figure 5 yields the energy dependence of the TICS for electron impact ionization of 1-butanol. The results from that analysis can be found in our accompanying paper [22]. Similarly, a Wannier threshold analysis [20,21] of those PICS might also yield the various appearance energies of the cationic fragments. That analysis can also be found in our companion paper to this investigation [22].

3. Results and Discussion

3.1 Mass Spectrum

The absolute mass spectrum of cations generated from dissociative ionization of 1-

butanol using incident electrons of 70 eV is shown in [figure 2](#). The electron impact with an electron energy at 70 eV is commonly studied, because this energy is sufficient for the spontaneous and stable fragmentation and the ion signals are most intense around 70 eV. A small change in the electron energy does not influence the fragmentation patterns. Furthermore, if the energy is decreased or increased substantially from 70 eV, the fragmentation is less stable and the intensity of the ion signal decreases notably. The mass spectrum of 1-butanol is important as it provides data to understand how the target molecule breaks down, and hence gives us the relative abundance, which allows us to understand which fragments are most likely to be formed from the ionization process. In this study we have assigned the identity of the cations assuming that all of the ions in the mass spectrum are singly ionized. That assumption is based on the premise that, in general, cross-sections for the formation of doubly-charged ions are, at least, one order of magnitude smaller than the cross sections for the formation of the singly-charged ions. It has previously been observed that doubly charged ion states, produced directly or indirectly through single ionization followed by auto-ionization, undergo fragmentation to multiple singly-charged ions [28,29]. This makes the observation of doubly charged fragments for molecules unlikely, as they can readily relax to produce multiple singly-charged fragments. For instance, in principle, doubly-ionized 1-butanol could be detected in our experiment at 37 amu. However, the singly ionized parent peak has a relative abundance of 0.73 (see [table 1](#)) and so it would therefore be expected that the doubly ionized cation peak would appear with a relative abundance < 0.073 . The peak of relative abundance = 0.85 at 37 amu is therefore more probably due to the formation of C_3H^+ cations. In addition while the energy for double ionization of 1-butanol is unknown, it is certainly lower than the second ionization energy for 1-propanal at 27.0 eV [27]. No appearance potential for 37 m/z at around 27 eV is, however, observed [22] thereby providing further evidence in support of our assumption.

The relative abundances of the cations with respect to the base peak of CH_2OH^+ ($m/z = 31$ amu), as well as their standard deviations and background contributions are given in [table 1](#). The present data compares reasonably well with the values reported by NIST [30], Zavilopulo *et al.* [15] and Friedel *et al.* [14]. Here we have observed 29 cationic fragments with an abundance higher than 1%. The mass spectrum of 1-butanol falls into six distinct groups from mass range 1-3 amu, 12-19 amu, 26-33 amu, 37-45 amu, 50-59 amu and 70-74 amu. There are only 4 cations with a relative intensity above 50%, including the base peak. These masses are 31 amu, 41 amu, 43 amu and 56 amu, which represent about 56% of the total intensity recorded in the mass spectrum. Among the group of cations with masses from 26-33 amu, the cations having a mass of 31 amu, 29 amu, 28 amu and 27 amu are observed with higher intensity, whereas in the cation groups with masses of 37-45 amu and 50-59 amu, the cations of masses 41-43 amu and 55-56 amu show the most intensity. Considering the group of cations with the highest mass, the parent cation M ($m = 74$ amu) appears due to the ejection of an electron from a non-bonding orbital on the oxygen atom having an ionization potential of 10.10 eV [31]. A peak of very small

intensity is also observed at 75 amu, which is attributed to a M+1 cation. The intensity of this peak is ~ 5% of the parent cation, and therefore is consistent with the natural abundance of the ^{13}C isotope. A successive loss of hydrogen from M is observed by the production of the fragments of masses between 73 and 65 amu. The cation of mass 61 amu ($\text{C}_3\text{H}_9\text{O}^+$) could be attributed to propyloxonium, produced by the loss of CH (methylidyne radical), and the cations $\text{C}_3\text{H}_8\text{O}^+$ (m = 60 amu), $\text{C}_3\text{H}_7\text{O}^+$ (m = 59 amu) and $\text{C}_3\text{H}_6\text{O}^+$ (m = 58 amu) are produced with the loss of CH_2 , CH_3 and CH_4 , respectively. The cations with masses in the range from 57 - 52 amu may be formed due to, besides the loss of CH_4 , the successive loss of hydrogen from $\text{C}_3\text{H}_6\text{O}^+$. Note that, in the region from 57 amu to 52 amu of the mass spectrum, the identity of the cation cannot be determined solely from the m/z ratio, given that some masses may be assigned to different molecules. For example, in both C_4H_9^+ and $\text{C}_3\text{H}_5\text{O}^+$ the masses are 57 amu. In this region (57 - 52 amu) there is also the formation of cations due to the successive loss of hydrogen from C_4H_9^+ , m = 57 amu, to C_4^+ , m = 48 amu. The cation C_4H_8^+ at 56 amu is the most prominent one and corresponds to the loss of a water molecule from the alcohol. Considering the third group of masses, which is dominated by cations at 41 and 43 amu, the mass 47 amu corresponds to the ethyloxonium ($\text{C}_2\text{H}_7\text{O}^+$) cation, involving the cleavage of the C_2 - C_3 bond, while the masses in the range 46 - 40 amu are produced by sequential loss of hydrogen from this cation. Again, a region of mass (between 44 - 40 amu) that corresponds to two different cations for each m/z ratio is observed. The intensity of the mass at 44 amu could be attributed to formation of both $\text{C}_2\text{H}_4\text{O}^+$ or C_3H_8^+ , and from this mass (44 amu) also occurs the formation of a series of cations from 44 down to 36 amu, due to the loss of hydrogen from C_3H_8^+ . The high intensity of the peak associated to the cation with 43 amu may be due to the formation of the complementary fragment oxonium with mass 31 amu. The same structure of cation formation is observed in the region from 35 amu to 24 amu, that is, a group of masses are formed by the sequential loss of hydrogen from CH_7O^+ . This group contains the base peak at 31 amu, a signature of all the primary alcohols, due to the cleavage of the C_1 - C_2 bond to give $\text{CH}_2=\text{OH}^+$, the oxonium ion. Again, the cation identity based on the mass alone, from 30 - 28 amu, is not unique. Cations in this region could also be formed by loss of hydrogen from ethane ions, C_2H_6^+ (m/z=30) to C_2^+ (m/z=24). Finally the low mass cations which are present in the mass spectra from all alcohols studied [20,21], can be attributed to the hydronium ion (H_3O^+) caused by the protonation, i.e., interaction of H_2O^+ and a proton H^+ , as well as the H_2O^+ cation at 18 amu, CH_3^+ cation at 15 amu and H_2^+ and H^+ at 2 and 1 amu, respectively.

3.2 Partial Ionization Cross Sections (PICS)

The absolute mass spectra, with the respective errors, for the primary alcohols from 1 to 3 carbons [20,21], are shown in the table 2 in comparison with the current data for 1-butanol. All these results again relate to an incident electron energy of 70 eV. This comparison has been possible by normalising the sum of all cations detected to the absolute total ionisation cross sec-

tions found in the literature [11, 24] at that energy. For all mass spectra recorded, the most intense peak is observed for the resonance-stabilized oxonium ion ($\text{CH}_2\text{O}^+\text{H}$) with mass 31 amu. The data in table 2 show a notable difference in the values of the PICS (70 eV), for three cations in the range of mass from 1 to 32 amu, as shown in figure 3. The cited masses are 15, 18 and 31 amu which correspond to the CH_3^+ , H_2O^+ and CH_2OH^+ ions, respectively. The ionic fragmentation of methanol provides the PICS (70 eV) for CH_3^+ by loss of OH ($m=17$ amu), whereas the ethanol, 1-propanol and 1-butanol lose CH_3O ($m = 31$ amu), $\text{C}_2\text{H}_5\text{O}$ ($m = 45$ amu) and $\text{C}_3\text{H}_7\text{O}$ ($m = 59$ amu), respectively. As the cations for the mass 17 amu, 31 amu, 45 amu and 59 amu also are shown in the relevant mass spectra, these processes probably occur by the carbon-carbon bond cleavage, where the formation of CH_3^+ is more effective from methanol. Similarly, the dehydration process (loss of H_2O) of these alcohols results in the formation of the ions CH_2^+ ($m = 14$ amu), C_2H_4^+ ($m = 28$ amu), C_3H_6^+ ($m = 42$ amu) and C_4H_8^+ ($m = 56$ amu). Although the production of both pairs of cations was observed in each process, formation of H_2O^+ is more effective when occurring through ionic fragmentation of ethanol. This PICS is about 60% more in magnitude than those of 1-butanol and 1-propanol and almost 93% higher than that of methanol. All four alcohols show CH_3O^+ as the most intense peak. The absolute cross section at 70 eV for this peak in 1-butanol is higher than that of methanol [20], slightly smaller than that of ethanol [20] and almost half that of the 1-propanol [21] case.

The corresponding fragments from the sigma-bond cleavage are those that produce CH_3O ($m/z = 31$ amu) are H^+ ($m/z = 1$ amu) for methanol, CH_3^+ ($m/z = 15$ amu) for ethanol, C_2H_5^+ ($m/z = 29$ amu) for propanol and C_3H_7^+ ($m/z = 43$ amu) for butanol. In table 2 it is possible to see that the relative abundance for these respective fragments is increasing as the fragment mass increases, indicating the relative stability of the relevant cations. The actual abundances relative to the most intense fragment here are ~ 5% (H^+), 10% (CH_3^+), 13% (C_2H_5^+), and 55% (C_3H_7^+). When the abundances (at 70 eV) of both fragments produced in this cleavage are summed, it is observed that this value increases with the carbon number until C_3 , whereas the value for 1-butanol is smaller than that for 1-propanol. This is due to the other appreciable cleavages, shown in figure 4 by the intensity of the peaks for the masses 41, 43 and 56 amu. Furthermore, the comparison between the production for the parent cations indicates that for both the PICS (at 70 eV) and the relative abundance, these values are decreasing when the carbon number is increasing from C_1 to C_4 . Thus the single ionization cross section of the parent of the 1-butanol molecule is smaller than those of the corresponding methanol, ethanol and 1-propanol parent species. This indicates that the fragmentation process is more spontaneous for the higher-order molecules.

The absolute partial ionization cross sections (PICS) were measured for 38 cations of 1-butanol in the energy range 10-100 eV, as shown in the table 3 and plotted in figure 5. These 38 fragment cations represent 96.6 % of the total ion abundance in the mass spectra generated by electrons with impact energy 70 eV. The PICS for the cations of masses 65 amu and 67-71 amu

are not included here because of their low abundance and high background, $\sim 57\text{-}75\%$, contribution. The absolute PICS of the lighter fragments, for example, H^+ and H_2^+ , were also excluded, because it was too difficult to obtain accurate results for them with the mass spectrometer used in our experiment. The PICS of the masses from 16-24 amu have also not been reported here, because of their low abundances in the mass spectrum and also because the masses at 17 amu and 18 amu have high backgrounds, 53.87% and 56.11% respectively. The absolute PICS of the individual cations of 1-butanol are shown in [figure 5](#), as noted above, where they all exhibit a similar energy dependence (i.e. cross section as a function of energy) and none indicate any structure. Note that these PICS can be summed to give the total ionization cross section for electron scattering from 1-butanol, which we undertake and then discuss what we find in detail in our companion paper [\[22\]](#).

4. Conclusions

This work reports on our measurements of the cation mass spectrum and absolute partial ionization cross sections, at 70 eV, from 1-butanol. Here we have shown 76 well-resolved mass peaks in the 1-75 amu mass range, in the mass spectrum, as well as their relative abundances and cation assignments. The present mass spectrum was found to be in pretty good agreement with the earlier data reported by NIST [\[30\]](#), Zavilopulo *et al.* [\[15\]](#) and Friedel *et al.* [\[14\]](#). The comparison between the absolute partial ionization cross sections of the primary alcohols from C_1 to C_4 , in our present and previous work, indicates some differences in the cross sections for like cations, thus providing more knowledge about the fragmentation process in each case. Among the primary alcohols of C_1 to C_4 , the 1-butanol molecule has been identified as one of the most promising to be used to replace fossil fuels. This follows as it can release more chemical energy, in the form of heat, during ignition and it will not need modifications to engine components if used instead of gasoline [\[4\]](#). Therefore, this study contributes with new experimental data that is required if we are to further understand and optimize the ignition process, required for the efficient and cost-competitive utilization of the primary alcohols as alternate fuels.

Acknowledgement

This work was supported by the Brazilian Conselho Nacional de Desenvolvimento Científico e Tecnológico (CNPq), Fundação de Amparo à Pesquisa do Estado de Minas Gerais (FAPEMIG) and FINEP. M.C.A.L., R.F.C.N. and H.V.D. acknowledge financial support from CNPq, while W.A.D. Pires, S. G., R.A.A.A. acknowledge the fellowship from CAPES. KLN would like to thank CNPq for an ‘Attracting Young Talent’ fellowship. One of us (MJB) also acknowledges financial support from the Australian Research Council (DP160102787).

References

- [1] A. K. Agarwal, *Progress in Energy and Combustion Science* **33** (2007) 2007.
- [2] S. Payne, T. Dutzik and E. Figdor, Environment America Research and Policy Center (2009). <http://www.environmentamerica.org/sites/environment/files/reports/The-High-Cost-of-Fossil-Fuels.pdf>.
- [3] M. A. Ridenti, J. A. Filho, M. J. Brunger, R. F. da Costa, M. T. do N. Varella, M. H. F. Bettega and M. A. P. Lima, *Eur. Phys. J. D* **70** (2016) 161.
- [4] M. J. Brunger, *Int. Rev. Phys. Chem.* **36** (2017) 333.
- [5] Biofuels the fuel of the future. <http://biofuel.org.uk/>.
- [6] B. Ndaba et al., *Biotechnology Reports* **8** (2015) 1–9.
- [7] Technology collaboration programme on advanced motor fuels: http://www.iea-amf.org/content/fuel_information/butanol/properties#octane_numbers
- [8] Wei-Qiang Han, Chun-De Yao, *Fuel* **150** (2015) 29–40.
- [9] P. Oßwald, H. Guldenberg, K. Kohse-Höinghaus, B. Yang, T. Yuan and F. Qi, *Combustion and Flame* **158** (2011) 2.
- [10] A. P. Mariano et al., *Biotechnology and Bioengineering* **108** (2011) 1757–1765.
- [11] J. E. Hudson, M. L. Hamilton, C. Vallance and P. W. Harland *Phys. Chem. Chem. Phys.* **5** (2003) 3162.
- [12] M. A. Khakoo, J. Muse, H. Silva, M. C. A. Lopes, C. Winstead, V. McKoy, E. M. de Oliveira, R. F. da Costa, M. T. do N. Varella, M. H. F. Bettega and M. A. P. Lima, *Phys. Rev. A* **78** (2008) 062714.
- [13] M. H. F. Bettega, C. Winstead and V. McKoy, *Phys. Rev. A* **82** (2010) 062709.
- [14] R. A. Friedel, J. L. Shultz, and A. G. Sharkey, *Anal. Chem.* **28** (1956) 926–934.
- [15] A. N. Zavilopulo, F. F. Chipev, L. M. Kokhtych, *Nucl. Instrum. Methods Phys. Res. B* **233** (2005) 302.
- [16] K. Fedus, C. Navarro, L. R. Hargreaves, M. A. Khakoo, F. M. Silva, M. H. F. Bettega, C. Winstead, and V. McKoy, *Phys. Rev. A* **90** (2014) 032708.
- [17] B. C. Ibănescu and M. Allan, *Phys. Chem. Chem. Phys.* **11** (2009) 7640.
- [18] H. Tanaka, M. J. Brunger, L. Campbell, H. Kato, M. Hoshino and A. R. P. Rau, *Rev. Mod. Phys.* **88** (2016), 025004.
- [19] L. Pitchford et al., *Plasma Process. Polym.* **14** (2017) 1600098.
- [20] K. L. Nixon, W. A. Pires, R. F. Neves, H. V. Duque, D. B. Jones, M. J. Brunger and M. C. Lopes, *Int. J. Mass. Spectrom.* **404** (2016) 48.
- [21] W. A. D. Pires, K. L. Nixon, S. Ghosh, R. F. C. Neves, H. V. Duque, R. A. R. Amorim, D. B. Jones, F. Blanco, G. García, M. J. Brunger and M. C. A. Lopes, *Int. J. Mass. Spectrom.* **422** (2017) 32.
- [22] S. Ghosh, K. L. Nixon, W. A. D. Pires, R. A. A. Amorim R. F. C. Neves, H. V. Duque, D. G. M. da Silva, D. B. Jones, F. Blanco, G. Garcia, M. J. Brunger and M. C. A. Lopes, *Int. J. Mass Spectrom.* (2018), companion paper.
- [23] Hiden Analytical: <http://www.hidenanalytical.com/en/>.
- [24] R. Rejoub, B. G. Lindsay, and R. F. Stebbings, *Phys. Rev. A* **65** (2002) 042713.
- [25] MDC Vacuum Products, <http://www.mdcvacuum.com>.
- [26] NIST WebBook: <http://webbook.nist.gov/cgi/cbook.cgi?ID=C71363&Mask=4&Type=ANTOINE&Plot=on>.
- [27] P. Linusson, M. Stenrup, Å. Larson, E. Andersson, F. Heijkenskjöld, P. Andersson, J. H. D. Eland, L. Karlsson, J.-E. Rubensson, and R. Feifel, *Phys. Rev. A* **80** (2009) 032516.
- [28] D.B. Jones, M. Yamazaki, N. Watanabe, M. Takahashi, *Phys. Rev. A* **86**, 062707 (2012).
- [29] D.B. Jones, M. Yamazaki, N. Watanabe, M. Takahashi, *Phys. Rev. A* **87**, 022714 (2013).
- [30] NIST WebBook: <http://webbook.nist.gov/cgi/cbook.cgi?ID=C71363&Mask=200>.
- [31] J. L. Holmes, F. P. Lossing, *Org. Mass Spectrom.* **26** (1991) 537.

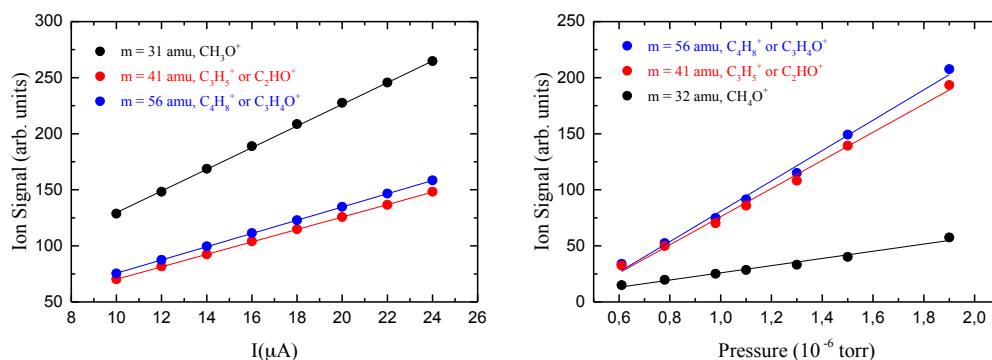


Figure 1: Linear dependencies between the operating pressure, the incident electron current and the detected ion signal in each case. Here the solid lines represent a linear fit to the experimental data points. a) Linear dependence of detected ion counts with incident electron current for the cations $m/z=31, 41, 56$ amu. b) Linear dependence of detected ion counts with pressure for the cations $m/z=56, 41, 32$ amu.

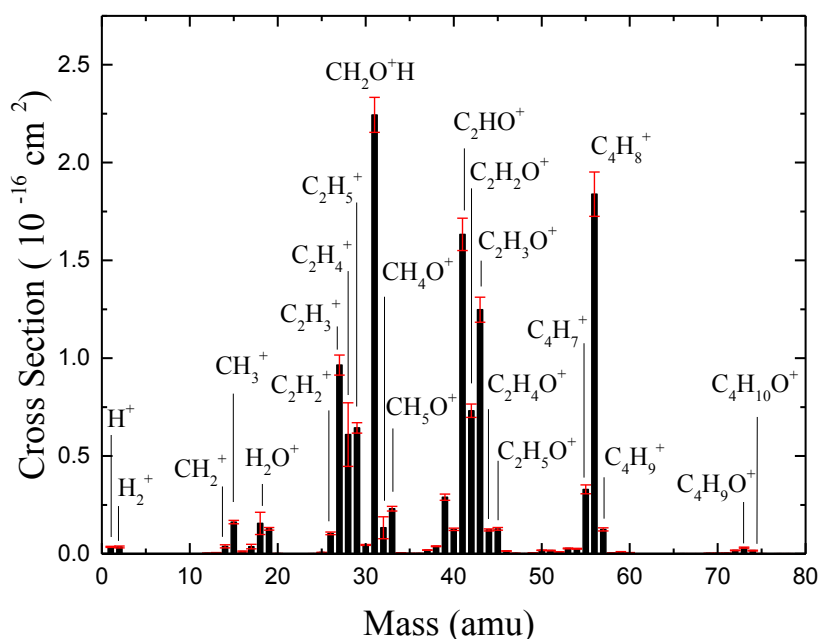


Figure 2: Mass spectrum of the cations generated from electron impact ionization of 1-butanol using incident electrons of 70 eV. Here the background spectrum was subtracted from the signal spectrum, taken on various days, and combined to produce a true spectrum. The data has been normalized to 100 for the most intense peak at $m/z=31$. Some suggestions as to the identity of the cations are also given, assuming all cations are singly ionized, with $M=74$ amu representing the parent cation: $\text{CH}_3\text{CH}_2\text{CH}_2\text{CH}_2\text{OH}^+$. Also shown on the plot are the error bars representing the standard deviation in the measured m/z and the uncertainty in the total ionization cross section [11], see text for details.

Table 1: Relative abundances of the cations generated by electron impact of 1-butanol using an electron energy of 70 eV. The relative abundances are expressed with respect to the most abundant cation, *i.e.* 31 amu. The present data are determined from the average of several measurements and the error is the standard deviation on that average. Also shown is the background contribution to measurements of 1-butanol, given as a percentage. The data from this study is compared with the corresponding data from other sources.

Cation Identity	M (amu)	Present Data			NIST [30]	Zavilopulo <i>et al.</i> [15]	R. A. Friedel <i>et al.</i> [14]
		Abundance	Error	% Background			
H ⁺	1	1.58	0.12	42.00			
H ₂ ⁺	2	1.56	0.20	16.56		5.88	
H ₃ ⁺	3	0.01	0.00	0			
C ⁺	12	0.12	0.01	4.42	0.3		
CH ⁺	13	0.25	0.03	1.67	0.85	2.21	
CH ₂ ⁺	14	1.70	0.41	4.11	3.05	8.44	
CH ₃ ⁺	15	7.22	0.26	1.39	10.46	40.69	
CH ₄ ⁺ or O ⁺	16	0.52	0.14	18.34	0.36	3.98	
OH ⁺	17	1.65	0.56	53.87	0.21	0.72	
H ₂ O ⁺	18	6.93	2.69	56.11	0.29	0.44	3.64
H ₃ O ⁺	19	5.69	0.20	0.68	4.48	3.70	3.53
H ₂ DO ⁺	20	0.06	0.02	24.49	0.07		
C ₂ ⁺	24	0.05	0.00	1.81			
C ₂ H ⁺	25	0.32	0.02	1.01			
C ₂ H ₂ ⁺	26	4.65	0.23	0.69	13.6	17.06	
C ₂ H ₃ ⁺	27	43.00	1.50	0.36	57.03	67.31	59.05
CO ⁺ or C ₂ H ₄ ⁺	28	27.17	8.90	4.69	19.67	30.22	20.51
COH ⁺ or C ₂ H ₅ ⁺	29	28.68	0.36	1.00	38.46	40.33	36.03
CH ₂ O ⁺ or C ₂ H ₆ ⁺	30	2.03	0.08	0.79	0.02	2.29	2.99
CH ₂ OH ⁺	31	100	0.00	0.04	98.13	100	100
CH ₄ O ⁺	32	5.94	3.16	4.36	2.16	36.02	1.81
CH ₅ O ⁺	33	10.28	0.35	0.04	9.07	2.98	7.52
CH ₆ O ⁺	34	0.23	0.01	1.82	0.23		
CH ₇ O ⁺	35	0.06	0.00	0.18			
C ₃ ⁺	36	0.07	0.00	4.77			
C ₃ H ⁺	37	0.85	0.03	0.58	2.59	6.24	
C ₃ H ₂ ⁺	38	1.71	0.06	0.68	6.35	9.42	
C ₃ H ₃ ⁺	39	12.90	0.49	0.71	25.43	22.53	
C ₂ O ⁺ or C ₃ H ₄ ⁺	40	5.59	0.15	0.68	0.23		
C ₂ HO ⁺ or C ₃ H ₅ ⁺	41	72.78	2.24	0.54	87.67	39.28	62.75
C ₂ H ₂ O ⁺ or C ₃ H ₆ ⁺	42	32.60	0.78	0.32	43.28	8.37	31.46
C ₂ H ₃ O ⁺ or C ₃ H ₇ ⁺	43	55.62	1.77	0.76	68.42	21.09	59.39
C ₂ H ₄ O ⁺ or C ₃ H ₈ ⁺	44	5.44	0.11	1.68	4.96	1.80	4.62
C ₂ H ₅ O ⁺	45	5.68	0.19	0.34	7.71	12.75	7.06
C ₂ H ₆ O ⁺	46	0.64	0.04	0.75	0.60	2.98	0.52
C ₂ H ₇ O ⁺	47	0.11	0.00	1.88			
C ₄ ⁺	48	0.03	0.01	4.61			
C ₄ H ⁺	49	0.20	0.01	1.34			
C ₄ H ₂ ⁺	50	0.79	0.05	2.90			
C ₄ H ₃ ⁺	51	0.75	0.05	3.50			
C ₄ H ₄ ⁺ or C ₃ O ⁺	52	0.42	0.04	2.74			
C ₄ H ₅ ⁺ or C ₃ HO ⁺	53	1.24	0.07	2.34			
C ₄ H ₆ ⁺ or C ₃ H ₂ O ⁺	54	1.15	0.09	1.99			
C ₄ H ₇ ⁺ or C ₃ H ₃ O ⁺	55	14.68	0.82	1.71	27.95	7.73	12.15
C ₄ H ₈ ⁺ or C ₃ H ₄ O ⁺	56	81.93	3.84	0.18	100	41.82	85.86
C ₄ H ₉ ⁺ or C ₃ H ₅ O ⁺	57	5.55	0.27	7.29	7.60	5.19	6.39
C ₃ H ₆ O ⁺	58	0.17	0.02	12.21	0.24		0.18
C ₃ H ₇ O ⁺	59	0.33	0.16	1.06	0.17		0.31
C ₃ H ₈ O ⁺	60	0.16	0.14	2.29			0.31
C ₃ H ₉ O ⁺	61	0.01	0.01	9.35			
C ₄ HO ⁺	65	0.01	0.00	72.82			
C ₄ H ₂ O ⁺	66	0.02	0.00	29.18			
C ₄ H ₃ O ⁺	67	0.01	0.01	75.98			
C ₄ H ₄ O ⁺	68	0.01	0.01	65.74			
C ₄ H ₅ O ⁺	69	0.09	0.02	57.21			0.09
C ₄ H ₆ O ⁺	70	0.12	0.03	59.46	0.03	0.39	0.11
C ₄ H ₇ O ⁺	71	0.13	0.03	64.38	0.12	1.52	0.11
C ₄ H ₈ O ⁺	72	0.78	0.06	3.43			0.11
C ₄ H ₉ O ⁺	73	1.39	0.11	0.62	1.52	5.19	1.39
C ₄ H ₁₀ O ⁺	74	0.73	0.08	1.73	0.74	3.01	0.74
¹² C ₃ ¹³ CH ₁₀ O ⁺	75	0.04	0.01	16.79	0.03	0.44	

Table 2: Absolute partial ionization cross sections (PICS) of the cations generated by electron impact of 1-butanol using an electron energy of 70 eV. The present data from 1-butanol are compared with those from methanol, ethanol and 1-propanol of our previous work [20,21].

Cation Identity	m	PICS (10^{-16} cm^2)							
		Methanol	error	Ethanol	error	1-propanol	error	1-butanol	error
H ⁺	1	0.0837	0.0118	0.0640	0.0130	0.0427	0.0108	0.0353	0.0030
H ₂ ⁺	2	0.0351	0.0079	0.0283	0.0088	0.0320	0.0073	0.0349	0.0046
C ⁺	12	0.0151	0.0012	0.0113	0.0009	0.0051	0.0014	0.0027	0.0002
CH ⁺	13	0.0271	0.0024	0.0362	0.0031	0.0115	0.0029	0.0056	0.0006
CH ₂ ⁺	14	0.0880	0.0110	0.1135	0.0097	0.0567	0.0144	0.0380	0.0080
CH ₃ ⁺	15	0.4858	0.0366	0.2829	0.0231	0.1823	0.0483	0.1619	0.0086
CH ₄ ⁺ or O ⁺	16	0.0185	0.0011	0.0219	0.0018	0.0114	0.0039	0.0117	0.0027
OH ⁺	17	0.0170	0.0143	0.0855	0.0155	0.0340	0.0198	0.0369	0.0119
H ₂ O ⁺	18	0.0243	0.0480	0.3599	0.0401	0.1426	0.0876	0.1554	0.0570
H ₃ O ⁺	19	0.0099	0.0006	0.1559	0.0135	0.0702	0.0144	0.1276	0.0067
H ₂ DO ⁺	20	0.0065	0.0004			0.0026	0.0005	0.0012	0.0004
C ₂ ⁺	24			0.0052	0.0004	0.0025	0.0002	0.0010	0.0001
C ₂ H ⁺	25			0.0299	0.0020	0.0170	0.0015	0.0070	0.0004
C ₂ H ₂ ⁺	26			0.1680	0.0112	0.1440	0.0107	0.1042	0.0066
C ₂ H ₃ ⁺	27			0.4687	0.0303	0.6031	0.0439	0.9650	0.0513
CO ⁺ or C ₂ H ₄ ⁺	28	0.1948	0.1246	0.2448	0.0616	0.5411	0.1518	0.6097	0.1626
COH ⁺ or C ₂ H ₅ ⁺	29	0.8215	0.0527	0.5288	0.0384	0.7183	0.0699	0.6435	0.0269
CH ₂ O ⁺ or C ₂ H ₆ ⁺	30	0.1551	0.0116	0.1601	0.0104	0.1210	0.0154	0.0455	0.0025
CH ₂ OH ⁺	31	1.6430	0.0985	2.6470	0.1588	5.5261	0.3868	2.2439	0.0897
CH ₄ O ⁺	32	1.2544	0.0795	0.1858	0.0577	0.2972	0.1183	0.1332	0.0559
CH ₅ O ⁺	33	0.0213	0.0012			0.0648	0.0047	0.2306	0.0121
CH ₆ O ⁺	34							0.0051	0.0003
CH ₇ O ⁺	35							0.0013	0.0001
C ₃ ⁺	36					0.0037	0.0004	0.0016	0.0001
C ₃ H ⁺	37					0.0244	0.0027	0.0191	0.0009
C ₃ H ₂ ⁺	38					0.0402	0.0047	0.0383	0.0020
C ₃ H ₃ ⁺	39					0.1614	0.0175	0.28944	0.0159
C ₂ O ⁺ or C ₃ H ₄ ⁺	40					0.0614	0.0084	0.1254	0.0060
C ₂ HO ⁺ or C ₃ H ₅ ⁺	41			0.0206	0.0029	0.2945	0.0330	1.6332	0.0825
C ₂ H ₂ O ⁺ or	42			0.0614	0.0041	0.6328	0.0670	0.7315	0.0341
C ₃ H ₆ ⁺									
C ₂ H ₃ O ⁺ or	43			0.1797	0.0117	0.1079	0.0119	1.2479	0.0639
C ₃ H ₇ ⁺									
C ₂ H ₄ O ⁺ or	44			0.0399	0.0027	0.0173	0.0070	0.1220	0.0054
C ₃ H ₈ ⁺									
C ₂ H ₅ O ⁺	45			1.0558	0.0685	0.0900	0.0393	0.1275	0.0066
C ₂ H ₆ O ⁺	46			0.5442	0.0831	0.0184	0.0192	0.0142	0.0010
C ₂ H ₇ O ⁺	47			0.0158	0.0023	0.0007	0.0005	0.0023	0.0001
C ₄ ⁺	48							0.0007	0.0001
C ₄ H ⁺	49							0.0045	0.0003
C ₄ H ₂ ⁺	50							0.0177	0.0012
C ₄ H ₃ ⁺	51							0.0167	0.0013
C ₄ H ₄ ⁺ or	52					0.0008	0.0001	0.0093	0.0009
C ₃ O ⁺									
C ₄ H ₅ ⁺ or	53					0.0062	0.0005	0.0277	0.0019
C ₃ HO ⁺									
C ₄ H ₆ ⁺ or	54					0.0012	0.0002	0.0258	0.0021
C ₃ H ₂ O ⁺									
C ₄ H ₇ ⁺ or	55					0.0124	0.0010	0.3293	0.0226
C ₃ H ₃ O ⁺									
C ₄ H ₈ ⁺ or	56					0.0044	0.0006	1.8385	0.1133
C ₃ H ₄ O ⁺									
C ₄ H ₉ ⁺ or	57					0.0373	0.0043	0.1246	0.0079
C ₃ H ₅ O ⁺									
C ₃ H ₆ O ⁺	58					0.0267	0.0025	0.0037	0.0004
C ₃ H ₇ O ⁺	59					0.4152	0.0397	0.0073	0.0035
C ₃ H ₈ O ⁺	60					0.2924	0.0362	0.0036	0.0030
C ₃ H ₉ O ⁺	61					0.0110	0.0014	0.0002	0.0001
C ₄ HO ⁺	65							0.0002	0.0001
C ₄ H ₂ O ⁺	66							0.0004	0.0001
C ₄ H ₃ O ⁺	67							0.0003	0.0002
C ₄ H ₄ O ⁺	68							0.0002	0.0001
C ₄ H ₅ O ⁺	69							0.0020	0.0003
C ₄ H ₆ O ⁺	70							0.0026	0.0006
C ₄ H ₇ O ⁺	71							0.0029	0.0006
C ₄ H ₈ O ⁺	72							0.0174	0.0016
C ₄ H ₉ O ⁺	73							0.0311	0.0027
C ₄ H ₁₀ O ⁺	74							0.0163	0.0019
¹² C ₃ ¹³ CH ₁₀ O ⁺	75							0.0008	0.0001

Table 3: Absolute partial ionization cross sections ($\times 10^{-16}$ cm²) for electron scattering from 1-butanol. The overall uncertainty on the data given below includes the uncertainty in the measurements of the mass spectrum and the error in normalizing to the absolute data of Hudson *et al.* [11]. The overall uncertainties in the PICS are presented in brackets and the mass units of each fragment are in amu.

Electron energy(eV)	74	73	72	60	59	58	57	56	55	54
	C ₄ H ₁₀ O ⁺ (12.6%)	C ₄ H ₉ O ⁺ (8.9%)	C ₄ H ₈ O ⁺ (9.2%)	C ₃ H ₈ O ⁺ (83.3%)	C ₃ H ₇ O ⁺ (48.7%)	C ₃ H ₆ O ⁺ (12.6%)	C ₄ H ₉ ⁺ or C ₃ H ₅ O ⁺ (6.4%)	C ₄ H ₈ ⁺ or C ₃ H ₄ O ⁺ (6.1%)	C ₄ H ₇ ⁺ or C ₃ H ₃ O ⁺ (6.8%)	C ₄ H ₆ ⁺ or C ₃ H ₂ O ⁺ (8.6%)
10	0	0	0	0	0	0	0	0.00002	0	0.00006
15	0.00437	0.00712	0.00529	0.00098	0.00165	0.00058	0.02643	0.50590	0.04275	0.00730
20	0.00932	0.01958	0.01074	0.00205	0.00476	0.00165	0.06861	1.16054	0.16919	0.01454
25	0.01216	0.02549	0.01364	0.00273	0.00629	0.00264	0.09445	1.49594	0.24528	0.01875
30	0.01404	0.02835	0.01518	0.00312	0.00687	0.00316	0.11079	1.66516	0.28429	0.02187
35	0.01510	0.02960	0.01609	0.00324	0.00734	0.00342	0.11955	1.76125	0.30475	0.02386
40	0.01586	0.03060	0.01671	0.00346	0.00752	0.00362	0.12378	1.81792	0.31716	0.02497
45	0.01633	0.03119	0.01708	0.00346	0.00761	0.00370	0.12589	1.85153	0.32387	0.02554
50	0.01644	0.03148	0.01710	0.00350	0.00747	0.00363	0.12714	1.86683	0.32936	0.02573
55	0.01656	0.03164	0.01759	0.00350	0.00756	0.00378	0.12715	1.87336	0.33213	0.02626
60	0.01666	0.03188	0.01759	0.00352	0.00749	0.00375	0.12613	1.87077	0.33249	0.02609
65	0.01651	0.03160	0.01775	0.00353	0.00729	0.00373	0.12560	1.85668	0.33224	0.02613
70	0.01639	0.03114	0.01742	0.00365	0.00732	0.00371	0.12465	1.83855	0.32937	0.02589
75	0.01632	0.03101	0.01731	0.00365	0.00744	0.00371	0.12320	1.81779	0.32679	0.02543
80	0.01639	0.03062	0.01703	0.00365	0.00741	0.00350	0.12145	1.78980	0.32086	0.02516
85	0.01585	0.03018	0.01670	0.00363	0.00727	0.00367	0.12011	1.76351	0.31678	0.02474
90	0.01570	0.02985	0.01628	0.00352	0.00730	0.00350	0.11934	1.73841	0.31250	0.02418
95	0.01551	0.02906	0.01620	0.00355	0.00731	0.00361	0.11823	1.72299	0.30746	0.02373
100	0.01544	0.02907	0.01594	0.00348	0.00713	0.00343	0.11760	1.70332	0.30343	0.02318

Electron energy(eV)	53	52	51	50	47	46	45	44	43	42
	C ₄ H ₅ ⁺ or C ₃ HO ⁺ (7.2%)	C ₄ H ₄ ⁺ or C ₃ O ⁺ (9.7%)	C ₄ H ₃ ⁺ (8.5%)	C ₄ H ₂ ⁺ (7.3%)	C ₂ H ₇ O ⁺ (7.1%)	C ₂ H ₆ O ⁺ (7.3%)	C ₂ H ₅ O ⁺ (5.2%)	C ₂ H ₄ O ⁺ (4.6%)	C ₂ H ₃ O ⁺ or C ₃ H ₇ ⁺ (5.2%)	C ₂ H ₂ O ⁺ or C ₃ H ₆ ⁺ (4.8%)
10	0	0	0	0	0	0	0	0	0.00001	0
15	0.00092	0.00215	0.00013	0.00014	0.00031	0.00249	0.00742	0.01514	0.14210	0.09917
20	0.00591	0.00393	0.00152	0.00069	0.00123	0.00790	0.04922	0.05661	0.60846	0.36448
25	0.01216	0.00508	0.00334	0.00191	0.00183	0.01092	0.08511	0.08525	0.90749	0.53168
30	0.01779	0.00600	0.00553	0.00335	0.00206	0.01248	0.10475	0.10337	1.06531	0.62180
35	0.02175	0.00697	0.00782	0.00532	0.00213	0.01305	0.11398	0.11326	1.15023	0.67220
40	0.02407	0.00779	0.01052	0.00747	0.00220	0.01361	0.11957	0.11785	1.19759	0.69988
45	0.02537	0.00833	0.01258	0.00986	0.00231	0.01388	0.12242	0.12263	1.21999	0.71601
50	0.02655	0.00878	0.01408	0.01259	0.00223	0.01409	0.12340	0.12059	1.23353	0.72485
55	0.02719	0.00893	0.01522	0.01464	0.00227	0.01423	0.12492	0.12184	1.24065	0.72981
60	0.02743	0.00915	0.01573	0.01589	0.00236	0.01416	0.12610	0.12174	1.24545	0.73210
65	0.02759	0.00946	0.01641	0.01711	0.00238	0.01442	0.12698	0.12185	1.24793	0.73247
70	0.02773	0.00936	0.01675	0.01779	0.00238	0.01427	0.12755	0.12208	1.24799	0.73157
75	0.02745	0.00935	0.01676	0.01872	0.00229	0.01433	0.12725	0.12177	1.24627	0.72964
80	0.02730	0.00919	0.01691	0.01909	0.00242	0.01445	0.12847	0.12126	1.24282	0.72558
85	0.02713	0.00912	0.01675	0.01933	0.00238	0.01454	0.12865	0.12097	1.23684	0.72165
90	0.02639	0.00881	0.01656	0.01935	0.00239	0.01449	0.12874	0.12024	1.22913	0.71589
95	0.02603	0.00863	0.01632	0.01932	0.00239	0.01437	0.12818	0.12035	1.22324	0.71048
100	0.02557	0.00848	0.01589	0.01901	0.00236	0.01428	0.12738	0.11873	1.21537	0.70408

Electron energy(eV)	41	40	39	38	37	33	32	31	30	29
	C ₂ HO ⁺ or C ₃ H ₅ ⁺ (5.1%)	C ₂ O ⁺ or C ₃ H ₄ ⁺ (5.0%)	C ₃ H ₃ ⁺ (5.6%)	C ₃ H ₂ ⁺ (5.4%)	C ₃ H ⁺ (5.5%)	CH ₅ O ⁺ (5.3%)	CH ₄ O ⁺ (4.2%)	CH ₂ OH ⁺ (4.0%)	CH ₂ O ⁺ or C ₂ H ₆ ⁺ (5.7%)	COH ⁺ or C ₂ H ₅ ⁺ (4.2%)
10	0.00006	0	0	0	0	0	0	0	0	0.00003
15	0.11786	0.01314	0.00273	0.00002	0	0.03915	0.01618	0.16945	0.00174	0.00705
20	0.61979	0.04637	0.01763	0.00033	0.00001	0.12853	0.05686	0.86880	0.00987	0.10996
25	1.04618	0.07177	0.05104	0.00103	0.00012	0.17737	0.08770	1.46416	0.02009	0.27044
30	1.30044	0.09122	0.10459	0.00259	0.00050	0.20119	0.10600	1.83345	0.02941	0.41242
35	1.44324	0.10563	0.16532	0.00611	0.00160	0.21320	0.11727	2.03885	0.03623	0.50963
40	1.52103	0.11396	0.21333	0.01161	0.00329	0.21953	0.12390	2.14598	0.04029	0.56827
45	1.56593	0.11920	0.24452	0.01851	0.00573	0.22261	0.12748	2.19891	0.04273	0.60333
50	1.59450	0.12161	0.26466	0.02522	0.00904	0.22518	0.12926	2.22413	0.04412	0.62358
55	1.61227	0.12367	0.27625	0.03010	0.01230	0.22702	0.13189	2.23675	0.04481	0.63516
60	1.62409	0.12475	0.28284	0.03352	0.01500	0.22925	0.13336	2.24315	0.04528	0.64021
65	1.62985	0.12507	0.28738	0.03642	0.01715	0.22967	0.13330	2.24505	0.04532	0.64242
70	1.63321	0.12548	0.28944	0.03833	0.01918	0.23061	0.13320	2.24397	0.04550	0.64358
75	1.63037	0.12516	0.29030	0.04000	0.02070	0.23224	0.13350	2.23982	0.04508	0.64209
80	1.62522	0.12480	0.28972	0.04100	0.02220	0.23336	0.13335	2.23098	0.04513	0.63842
85	1.61318	0.12365	0.28669	0.04183	0.02333	0.23408	0.13320	2.22529	0.04470	0.63263
90	1.60181	0.12232	0.28403	0.04217	0.02423	0.23415	0.13273	2.21217	0.04446	0.62821
95	1.58971	0.12149	0.28035	0.04220	0.02489	0.23513	0.13263	2.20542	0.04391	0.62351
100	1.57206	0.11952	0.27622	0.04187	0.02523	0.23338	0.13229	2.19384	0.04362	0.61531

Electron energy(eV)	28	27	26	25	15	14	13	12
	CO ⁺ or C ₂ H ₄ ⁺ (26.6%)	C ₂ H ₃ ⁺ (5.3%)	C ₂ H ₂ ⁺ (6.4%)	C ₂ H ⁺ (6.8%)	CH ₃ ⁺ (5.4%)	CH ₂ ⁺ (21.3%)	CH ⁺ (11.6%)	C ⁺ (11.9%)
10	0	0	0	0	0	0	0	0
15	0.02901	0.00136	0.00124	0	0.00062	0	0	0
20	0.18510	0.10641	0.00484	0.00008	0.00455	0.00050	0.00002	0
25	0.33288	0.31442	0.00987	0.00053	0.01425	0.00153	0.00009	0.00007
30	0.44502	0.53040	0.01958	0.00096	0.03513	0.00323	0.00025	0.00035
35	0.51660	0.70379	0.03546	0.00139	0.06523	0.00668	0.00057	0.00068
40	0.56200	0.81821	0.05164	0.00180	0.09440	0.01106	0.00100	0.00089
45	0.58863	0.88894	0.06711	0.00243	0.11670	0.01672	0.00156	0.00116
50	0.60199	0.92857	0.07938	0.00313	0.13327	0.02240	0.00234	0.00145
55	0.61230	0.95048	0.08871	0.00407	0.14546	0.02738	0.00312	0.00170
60	0.61593	0.96149	0.09584	0.00510	0.15335	0.03170	0.00393	0.00204
65	0.61231	0.96402	0.10064	0.00620	0.15839	0.03531	0.00502	0.00234
70	0.60977	0.96503	0.10429	0.00709	0.16195	0.03806	0.00566	0.00274
75	0.60282	0.95906	0.10714	0.00786	0.16365	0.04032	0.00649	0.00309
80	0.59577	0.94912	0.10749	0.00847	0.16447	0.04243	0.00715	0.00343
85	0.58830	0.93627	0.10843	0.00917	0.16408	0.04372	0.00777	0.00377
90	0.57901	0.92153	0.10819	0.00969	0.16307	0.04461	0.00832	0.00406
95	0.56884	0.90779	0.10754	0.01006	0.16158	0.04477	0.00887	0.00439
100	0.56229	0.88956	0.10653	0.01045	0.15967	0.04537	0.00929	0.00462

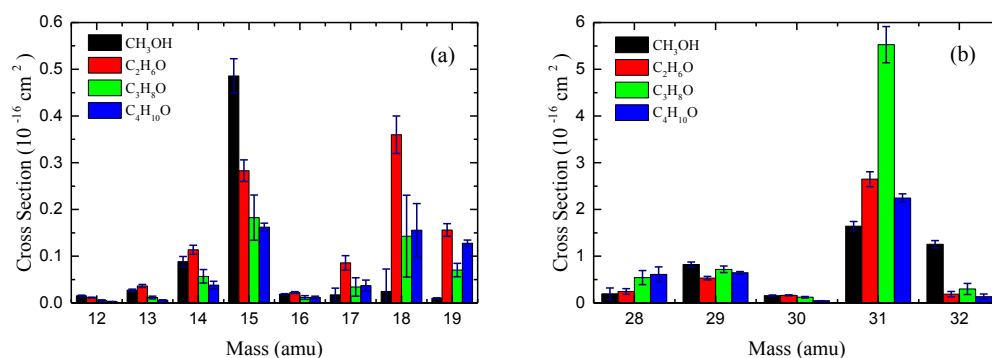


Figure 3: Absolute mass spectrum of the cations generated from electron impact ionization of methanol, ethanol, 1-propanol and 1-butanol using incident electrons of 70 eV, (a) for masses in the range 12–19 amu and (b) for masses in the range 28–32 amu. Here the background spectrum was subtracted from the signal spectrum to produce a true spectrum. The data of 1-butanol has been normalized using the absolute value of the total ionisation cross section (TICS) from Hudson *et al.* [11]. The present error bars were obtained by also considering the error on the data from Hudson *et al.* [11].

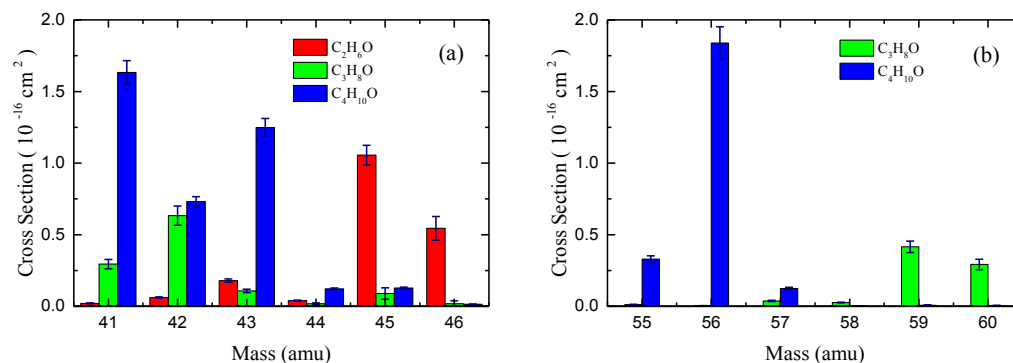


Figure 4: Absolute mass spectrum of the cations generated from electron impact ionization of ethanol, 1-propanol and 1-butanol using incident electrons of 70 eV. (a) for masses in the range 41–46 amu and (b) for masses in the range 55–60 amu. Here the background spectrum was subtracted from the signal spectrum to produce a true spectrum. The data of 1-butanol has been normalized using the absolute value of the TICS from Hudson *et al.* [11]. The present error bars were obtained by also considering the error on the data from Hudson *et al.* [11].

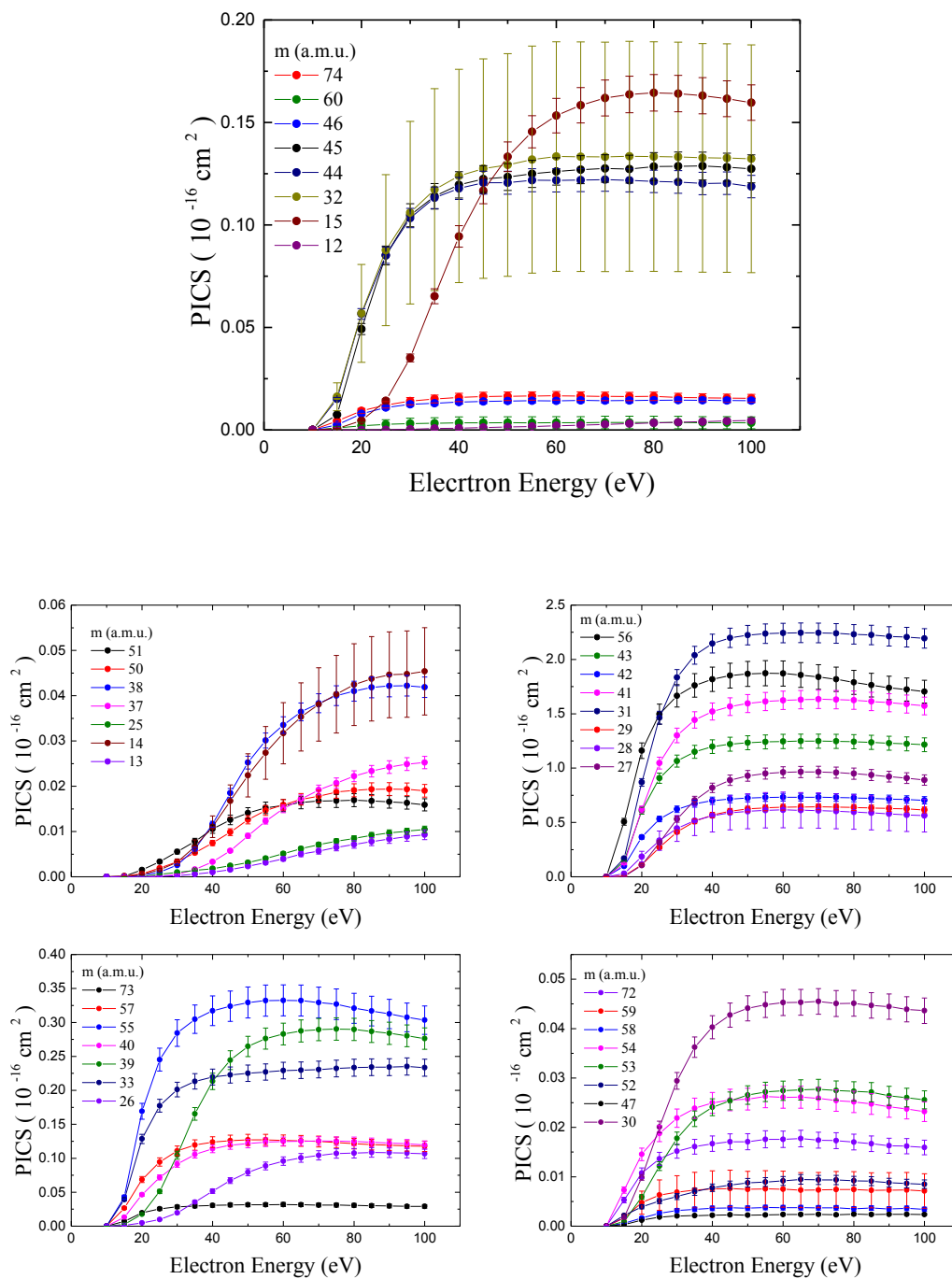


Figure 5: Absolute partial ionization cross sections (PICS) of the main 38 cations that result from electron impact ionization of 1-butanol, as measured in the present study. The errors are the quadrature sum of (i) the uncertainty in the experimental measurements of the cross sections, (ii) the uncertainty of the relative contributions to the mass spectrum and (iii) the normalization to the absolute data of Hudson *et al.* [11].